

Process Variation Aware Modeling of Interconnect Capacitance

Yu Bi[†], D. Ioan[‡], N.P. van der Meijs[†]

[†] EEMCS, Delft University of Technology, Mekelweg 4, Delft, The Netherlands (Email: y.bi@tudelft.nl)

[‡] NML, Politechnica University of Bucharest, Spl. Independentei 313, Bucharest, Romania (Email: daniel@lmm.pub.ro)

Abstract—We describe an efficient sensitivity method to model interconnect capacitances considering process variations. By using the so-called adjoint technique, the capacitance sensitivities w.r.t. multiple geometric parameters can come along with one time 3d capacitance extraction using the Boundary Element Method (BEM). Both theoretical and experimental examples are given to demonstrate the modeling method.

Index Terms—Interconnects, capacitances, variability, sensitivity.

I. INTRODUCTION

The on-going reduction of feature size goes together with an increase of variability. Obviously, there are more technological opportunities for aggressive scaling when more variability can be tolerated. This will lead to better and cheaper products (provided the quantities are large enough). Therefore, while the challenge of the technologists is to realize scaling while controlling the variability and the challenge of designers is to make the resulting variability sufficiently harmless by using suitable architectures and topologies, the challenge of Electronic Design Automation (EDA) is to provide accurate and efficient procedures to enable designers to understand the effect of the pertinent process variability on their design.

Accurate capacitance extraction is essential for signal integrity analysis of IC interconnects. However, the increasing process variations can affect electrical parameters of interconnects (e.g. capacitances) and further influence circuit performance and functionality. Therefore it is very important to capture such effects using an efficient model, which can be integrated in current design flow or verification methodology at a modest computation cost.

Our study focuses on the dimensional variations of interconnects. It has been shown that not all variations are fatal for capacitances [1]. For each capacitance, some geometric variations deserve further study and modeling while others can be simply neglected. First-order capacitance sensitivities w.r.t. these geometric parameters can be used to setup the threshold for making this distinction.

As a simple illustration, we assume a capacitance C being a function of only one geometric parameter x (e.g. the width of an interconnect or the thickness of a dielectric layer), denoted $C = f(x)$. It is introduced in [1] that the statistical approach and the deterministic approach can be related as in the following equation:

$$\frac{\sigma_C}{C_0} \approx \frac{1}{C_0} \left| \frac{df}{dx}(x_0) \right| \frac{\sigma_x}{x_0} \quad (1)$$

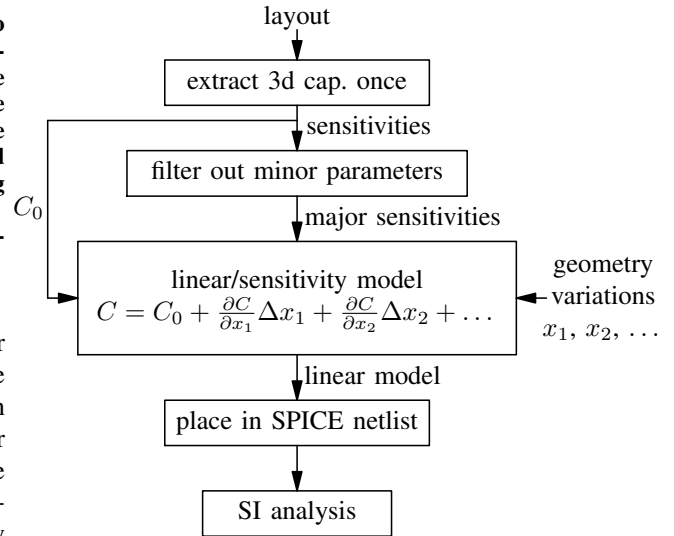


Fig. 1. Illustration of the steps from interconnect layout to signal integrity analysis using linear models of capacitances.

where x_0 and C_0 are the mean values of x and C ; σ_x and σ_C are their standard deviations, respectively. $\left| \frac{df}{dx}(x_0) \right|$ is the first-order sensitivity of C w.r.t. parameter x at its mean value x_0 . By using this equation, we can easily distinguish the “fatal” or major parameters resulting in large-deviation of C from the other parameters having minor effects on C (i.e. generating small-deviation of C), as long as we can compute the sensitivities w.r.t. all parameters with a modest complexity.

After filtering out the minor parameters, we need to capture the effects of the major parameters. Given the information of dimensional variations, a linear model of capacitances as a function of geometric parameters can be constructed and placed in the SPICE netlist instead of the nominal capacitances [2]. Subsequent signal integrity analyses can then be conducted, e.g. moment-based timing analysis [3], [4]. Figure 1 illustrates how our proposed method can be implemented in the current design flow. Note that although for simplicity reasons, we only consider capacitances here, resistances can easily be integrated in a similar way.

We have two tasks to accomplish. One is to generally prove that first-order approximation of capacitance is sufficient enough, which has been shown in [5]. The other is the main goal of this paper: to compute the first-order sensitivities accurately and efficiently.

We have presented an algorithm based on the Adjoint Field Technique (AFT) to calculate sensitivities of coupling capacitances w.r.t. geometric parameters and verified it with 2d experiments [6]. This paper is an extension and summary of our previous work. Some necessary background information are given in Section II. Section III derives the sensitivity computation for both ground capacitances and coupling capacitances for completeness and ease of interpretation. Analytical and numerical examples, both in 3d, are given in Section IV. Finally, Section V concludes the paper.

II. BACKGROUND

The capacitances that are used in SPICE netlists for signal integrity analysis of IC interconnects are actually called the *two-terminal capacitances* or *network capacitances* defined as

$$C_{ij} = Q_{ij}/(V_i - V_j)$$

where $C_{ij} = C_{ji}$ is the coupling capacitance between conductor i and j , V_i is the potential of conductor i and Q_{ij} the charge associated with this capacitance [7].

Assume that there are N conductors in a charge-free domain Ω , the relation between network capacitances, charges and voltages can be expressed in matrix notation:

$$\mathbf{Q} = \mathbf{C}_s \mathbf{V}$$

where \mathbf{Q} and \mathbf{V} are $N \times 1$ vectors, representing the charges and the potentials on N conductors. \mathbf{C}_s is an $N \times N$ matrix whose entry C_{sij} is the so-called *short-circuit capacitance* [7]. It equals the charge on conductor i when conductor j is held at a unit potential and all other conductors are short-circuited to ground. It can be shown that \mathbf{C}_s is symmetrical and positive definite. Multiplying by \mathbf{C}_s^{-1} on both sides of the equation generates

$$\mathbf{V} = \mathbf{C}_s^{-1} \mathbf{Q} = \mathbf{G} \mathbf{Q}$$

where \mathbf{G} is an $N \times N$ matrix of which the entry G_{ij} is given by the Green's function between conductor i and j .

In fact, network capacitances are specified in terms of the short-circuit capacitances based on the following relationship:

$$\begin{aligned} C_{ij} &= -C_{sij} \quad \forall i \neq j; \\ C_{ii} &= \sum_{j=1}^N C_{sij} \quad \forall i = 1, 2, \dots, N \end{aligned} \quad (2)$$

where C_{ii} is the ground (network) capacitance and the short-circuit capacitances are given by the inverse of the Green's function matrix ($\mathbf{C}_s = \mathbf{G}^{-1}$).

When the Boundary Element Method (BEM) is used for capacitance extraction, conductors are discretised into panels. Each panel forms effectively a separate conductor assumed not to have galvanic (DC) coupling to any other panel. The short-circuit capacitances associated to the

discretised panels before their association to conductors are called *partial short-circuit capacitances* [7], denoted by \mathbf{c}_s in this paper. If there are in total m panels in the domain, \mathbf{c}_s becomes an $m \times m$ (usually $m \geq N$) matrix. Correspondingly, other electrical quantities for panels, instead of \mathbf{V} , \mathbf{Q} and \mathbf{G} , are denoted in lower case as well: $\mathbf{q} = \mathbf{c}_s \mathbf{v} = \mathbf{g}^{-1} \mathbf{v}$.

III. ALGORITHM DERIVATION

Our algorithm [6] is based on an adjoint technique derived from an application of Tellegen's theorem to the electrostatic (ES) field, which is expressed as

$$(\hat{\mathbf{V}}, (\Delta \mathbf{C}_s) \mathbf{V}) = \langle (\Delta \epsilon) \mathbf{E}, \hat{\mathbf{E}} \rangle \quad (3)$$

where we assume there are N conductors in domain Ω and use a notation “ $\hat{\cdot}$ ” for the adjoint field quantities. $\Delta \mathbf{C}_s$ and $\Delta \epsilon$ are the effective changes of \mathbf{C}_s and ϵ (the permittivity of the medium in domain Ω) induced by the variation in geometric parameter p (Δp).

Equation (3) shows that the effects of the geometric variations on capacitances can be measured by the effects on the permittivity. It is necessary to mention that (3) is derived under the condition that $\Delta \mathbf{V} = 0$, which means the excitation voltages are considered constant in our study.

First of all, let's study the left-hand side of (3). Given the relationship between network capacitances and short-circuit capacitances described in (2), if we want to calculate:

- 1) ΔC_{ii} , the change of the ground capacitance due to Δp , we need to define the excitation voltages of the original system and the adjoint system as

$$\begin{aligned} V_k &= 1 \quad (k = 1, 2, \dots, N) \\ \hat{V}_i &= 1, \quad \hat{V}_k = 0 \quad (k \neq i) \end{aligned}$$

Therefore the left-hand side of (3) becomes

$$(\hat{\mathbf{V}}, (\Delta \mathbf{C}_s) \mathbf{V}) = \sum_{j=1}^N \Delta C_{sij} = \Delta C_{ii}. \quad (4)$$

- 2) ΔC_{ij} , the change of the coupling capacitance due to the geometric variation Δp , we need to define

$$\begin{aligned} V_j &= 1, \quad V_k = 0 \quad (k \neq j) \\ \hat{V}_i &= 1, \quad \hat{V}_k = 0 \quad (k \neq i) \end{aligned}$$

In this case, the left-hand side of (3) turns to be

$$(\hat{\mathbf{v}}, (\Delta \mathbf{C}_s) \mathbf{V}) = \Delta C_{sij} = -\Delta C_{ij}. \quad (5)$$

Now let's look at the right-hand side of (3): $\langle (\Delta \epsilon) \mathbf{E}, \hat{\mathbf{E}} \rangle$, which implies that we need to study how the variation of geometric parameter Δp influences the ϵ in Ω .

We know that the electric displacement field \mathbf{D} represents how much an electric field \mathbf{E} influences the organization

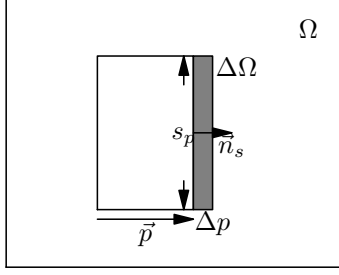


Fig. 2. Illustration of $\Delta\Omega$

of electrical charges in a medium characterized by the permittivity ϵ . In other words, the effect of \mathbf{E} is represented by \mathbf{D} via ϵ , and ϵ describes the relationship between \mathbf{E} and \mathbf{D} . While a perfect metal is placed in Ω , the inner part of the metal is actually shielded out, so there is no \mathbf{E} -field, nor its effect (\mathbf{D}) and their relationship (ϵ) exist anymore.

Figure 2 schematically shows the cross-section of a conductor when there is a variation in p (Δp). S_p is the influenced surface due to Δp and we call it the *victim surface* incident to parameter p . In fact, the dimensional variation Δp is exactly the displacement of the victim surface. The influence on ϵ lies on the shadowed area $\Delta\Omega$ where the effect of E-field is shielded out. Therefore $\Delta\epsilon\Delta\Omega = \epsilon(\vec{n}_p\Delta p)(\vec{n}_s\Delta s)$, where \vec{n}_s is pointing from the victim surface to the medium (characterized by ϵ) and \vec{n}_p is the direction of the geometric parameter we defined. Thus (3) becomes

$$\begin{aligned} (\hat{\mathbf{V}}, (\Delta\mathbf{C}_s)\mathbf{V}) &= \langle (\Delta\epsilon)\mathbf{E}, \hat{\mathbf{E}} \rangle = \int_{\Omega} (\Delta\epsilon)\mathbf{E}\hat{\mathbf{E}}d\Omega \\ &= \int_{s_p} \epsilon\mathbf{E}\hat{\mathbf{E}}(\vec{n}_p\Delta p)\vec{n}_s ds \end{aligned} \quad (6)$$

which will be used to calculate capacitance sensitivities categorized in two cases: sensitivity of ground capacitances and sensitivity of coupling capacitances.

Case-1 Ground capacitance sensitivity $\frac{\partial C_{ii}}{\partial p}$.

$$\begin{aligned} \frac{\partial C_{ii}}{\partial p} &= \lim_{\Delta p \rightarrow 0} \sum_{j=1}^N \Delta C_{s_{ij}} / \Delta p = \lim_{\Delta p \rightarrow 0} \int_{s_p} \frac{\epsilon\mathbf{E}\hat{\mathbf{E}}}{\Delta p} (\Delta p\vec{n}_p)\vec{n}_s ds \\ &= \epsilon\vec{n}_p\vec{n}_s \int_{s_p} \mathbf{E}\hat{\mathbf{E}} ds \end{aligned} \quad (7)$$

When the BEM is applied, \mathbf{E} is a piecewise constant (PWC) quantity on the set of panels. Hence, the integration over s_p becomes a summation. When also using $\mathbf{D} = \epsilon\mathbf{E}$ and $\nabla \cdot \mathbf{D} = \rho$ (Gauss law), the sensitivity expression becomes $\vec{n}_p\vec{n}_s \sum_{k \in s_p} \rho_k \hat{\rho}_k a_k / \epsilon$, where a_k is the corresponding area of panel k on the victim surface s_p . For panel k , since PWC is used for the BEM, the charge density ρ_k can be related to its charge q_k with the corresponding area a_k as $q_k = \rho_k a_k$. Consequently, the sensitivity expression transforms into $\vec{n}_p\vec{n}_s \sum_{k \in s_p} q_k \hat{q}_k / (a_k \epsilon)$. We know that q_k

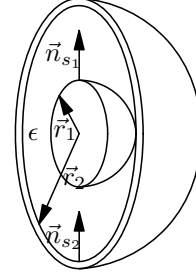


Fig. 3. Schematic diagram of concentric spheres.

and \hat{q}_k , as entries in \mathbf{q} , are certain combinations of some entries of the partial short-circuit capacitance matrix \mathbf{c}_s which is given by the inverse of the Green's function matrix \mathbf{g}^{-1} . According to (4), we have

$$q_k = \sum_{j=1}^N \sum_{a \in N_j} c_{sk,a}; \quad \hat{q}_k = \sum_{a \in N_i} c_{sk,a}. \quad (8)$$

with N_j being conductor j and $c_{sk,a}$ the short-circuit capacitance between panel k and a .

For ease of discussion, we introduce a short-hand notation: $C_{kj}^* = \sum_{a \in N_j} c_{sk,a}$. Therefore equation (7), the sensitivity of ground capacitance w.r.t. p becomes

$$\frac{\partial C_{ii}}{\partial p} = \frac{\vec{n}_p\vec{n}_s}{\epsilon} \sum_{k \in s_p} C_{ki}^* \left(\sum_{j=1}^N C_{kj}^* \right) / a_k. \quad (9)$$

Case-2 Coupling capacitance sensitivity $\frac{\partial C_{ij}}{\partial p}$. Similar to Case-1, according to (5), we finally obtain

$$\begin{aligned} \frac{\partial C_{ij}}{\partial p} &= -\frac{\vec{n}_p\vec{n}_s}{\epsilon} \sum_{k \in s_p} \left(\sum_{a \in N_i} \sum_{b \in N_j} c_{sk,a} c_{sk,b} \right) / a_k \\ &= -\frac{\vec{n}_p\vec{n}_s}{\epsilon} \sum_{k \in s_p} \frac{C_{ki}^* C_{kj}^*}{a_k}. \end{aligned} \quad (10)$$

From the above derivation we can see, similar to network capacitances (2), their sensitivities can also be computed from (partial) short-circuit capacitances (9), (10). In other words, with only one 3d capacitance extraction using the BEM (e.g. SPACE layout-to-circuit extractor [8]), we can obtain network capacitances as well as their sensitivities. Furthermore, multiple geometric parameters can be studied simultaneously. This is because they are associated to various victim surfaces, containing various sets of panels. Thus the sensitivities w.r.t. different parameters simply means different combinations of partial short-circuit capacitances in (8) and (10).

IV. EXAMPLES

Analytical Example In this subsection, we give an example of a system with two concentric spheres as is shown in Figure 3. We define the inner sphere as conductor 1 and the outer sphere conductor 2, while q_i, v_i ($i = 1, 2$) are

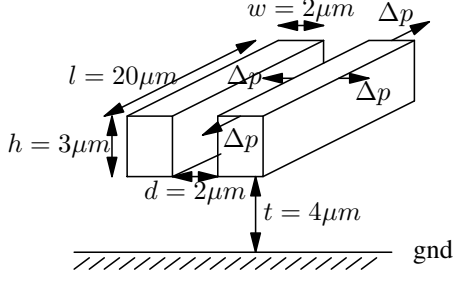


Fig. 4. Two parallel wires above the ground plane.

the corresponding charges and applied voltages on them. Analytically, the capacitance between the two spheres is $C_{12} = 4\pi\epsilon/(\frac{1}{r_1} - \frac{1}{r_2})$ and its sensitivities or derivatives w.r.t. r_1 and r_2 are $\frac{\partial C_{12}}{\partial r_1} = 4\pi\epsilon(r_2)^2/(r_2 - r_1)^2$ and $\frac{\partial C_{12}}{\partial r_2} = -4\pi\epsilon(r_1)^2/(r_2 - r_1)^2$.

Now we compute the sensitivities with our algorithm. Without loss of generality, we consider the inner sphere and the outer sphere to be a single panel each. So the area of each panel is $a_i = 4\pi r_i^2$ ($i = 1, 2$). According to the above analysis, the sensitivity of C_{12} against r_1 can be computed as $-q_1 \hat{q}_1 / (\epsilon a_1)$, where q_1 and \hat{q}_1 are the charges on the inner sphere when $V_1 = 0$, $V_2 = 1$ and $\hat{V}_1 = 1$, $\hat{V}_2 = 0$ respectively. Knowing that $q_1 = -\hat{q}_1 = -4\pi\epsilon/(\frac{1}{r_1} - \frac{1}{r_2})$, it is trivial to calculate the sensitivity of the coupling capacitance w.r.t. r_1 : $4\pi\epsilon(r_2)^2/(r_2 - r_1)^2$. Similarly the sensitivity of C_{12} w.r.t. r_2 can be calculated using our algorithm, resulting in $-4\pi\epsilon(r_1)^2/(r_2 - r_1)^2$. Note that when r_2 is the geometric parameter, $\vec{n}_p \vec{n}_s = \vec{n}_{r_2} \vec{n}_{s_2} = -1$. Apparently, our algorithm gives identical sensitivities as the analytical results.

We also studied a special case where there is one isolated sphere with a radius of r (we can also consider the radius of the outer sphere infinitely large). Analytically, the capacitance to the infinity (the reference ground) is $C_{gnd} = 4\pi\epsilon r$ and its sensitivity w.r.t. r is $4\pi\epsilon$.

The sensitivity of C_{gnd} computed by our algorithm is consistent with the analytical result:

$$\frac{dC_{gnd}}{dr} = \frac{\vec{n}_p \vec{n}_s q \hat{q}}{\epsilon a} = \frac{1}{\epsilon} \frac{C_{gnd}^2}{a} = \frac{1}{\epsilon} \frac{(4\pi\epsilon r)^2}{4\pi r^2} = 4\pi\epsilon \quad (11)$$

Numerical Examples An experiment is conducted on a system with two parallel wires above the ground plane, as shown in Figure 4. Assume there is a 10% variation in the layout ($\Delta p = 0.1\mu m$). Hence all the sidewalls of both conductors are victim surfaces.

The relative variability of the coupling capacitance C_{12} and the ground capacitance C_{gnd} can be computed via sensitivities given by our algorithm:

$$\begin{aligned} \frac{\Delta C_{12}}{C_{12}} &= \frac{\partial C_{12}}{\partial p} \times \frac{\Delta p}{C_{12}} = 9.35\%; \\ \frac{\Delta C_{gnd}}{C_{gnd}} &= \frac{\partial C_{gnd}}{\partial p} \times \frac{\Delta p}{C_{gnd}} = 1.43\%. \end{aligned} \quad (12)$$

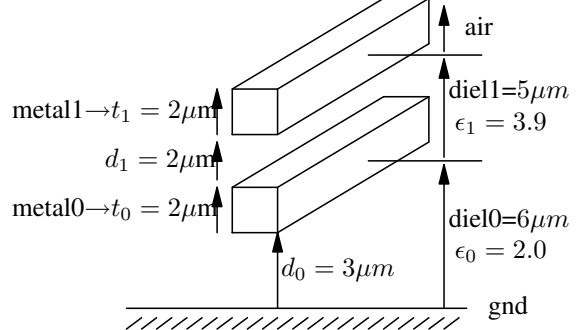


Fig. 5. Two wires one on top of the other.

To verify the accuracy of our algorithm, we change the layout by Δp and extract the capacitances again, denoting the results as C_{12}^p and C_{gnd}^p . Thus the actual relative variability of C_{12} and C_{gnd} are $(C_{12}^p - C_{12})/C_{12} = 10.94\%$ and $(C_{gnd}^p - C_{gnd})/C_{gnd} = 1.66\%$ respectively.

This experiment shows that for a $0.1\mu m$ geometric variation, our algorithm very nicely captures its effect on network capacitances. The coupling capacitance is very susceptible to variations in the layout, which needs to be modeled and integrated in the design flow. On the other hand, the ground capacitance, in this particular case, is not sensitive to layout variations.

Another experiment is conducted to study the vertical dimensional variations. As shown in Figure 5, there are two parallel wires one on top of the other. The width and the length of both wires are $2\mu m$ and $25\mu m$ respectively. Here we consider two geometric parameters, one being the distance between two wires d_1 and the other the distance between the lower wire and the ground denoted d_0 . d_1 and d_0 are independent parameters because they are related to difference manufacturing processes. Assume there is a $-0.2\mu m$ variation in both parameters. Hence the top surfaces and the bottom surfaces of both wires are all victim surfaces only they contribute different signs for ϵ as explained in Section III.

There are three network capacitances need to be considered in this system: the coupling capacitance C_{cp} and two ground capacitances C_{gnd1} (metal0 to ground), C_{gnd2} (metal1 to ground). Take the coupling capacitance for example. The linear model of C_{cp} in terms of d_1 and d_0 is written as follows:

$$C_{cp} = C_{cpo} + \frac{\partial C_{cp}}{\partial d_1} \times \Delta d_1 + \frac{\partial C_{cp}}{\partial d_0} \times \Delta d_0$$

Table I shows how much linear models can better approximate the capacitances considering process variations, compared to 0th-order models (simply neglecting variations).

V. CONCLUSION

To take into account process variabilities, we proposed a practical method to implement linear models of capaci-

TABLE I
 DEVIATIONS FROM ACTUAL CAPACITANCES GIVEN BY THE
 0th-ORDER AND THE 1st-ORDER MODELS RESPECTIVELY.

	Dev. C_{cp}	Dev. C_{gnd1}	Dev. C_{gnd2}
0th-order	14.22%	2.59%	3.96%
1st-order	1.24%	0.35%	0.29%

tances in standard circuit simulation and signal integrity analysis using first-order sensitivities. An algorithm was presented to compute these capacitance sensitivities w.r.t. geometric parameters. Both the network capacitances and their sensitivities can be obtained under only one time 3d extraction using the BEM. Analytical and numerical examples have been shown to verify our algorithm.

ACKNOWLEDGMENT

The authors would like to thank Juliusz Poltz from OptEM for his helpful comments. This work is in part supported by the EC (IST project-027378 CHAMELEON RF), the Dutch Technology Foundation STW (project 6913) and NXP Semiconductors in the context of the EMonIC project.

REFERENCES

- [1] T. El-Moselhy, I. M. Elfadel, and D. Widiger, "Efficient algorithm for the computation of on-chip capacitance sensitivities with respect to a large set of parameters," in *Proc. 45th ACM/IEEE Design Automation Conference DAC 2008*, pp. 906–911, 2008.
- [2] A. Labun, "Rapid method to account for process variation in full-chip capacitance extraction," *IEEE Trans. Comput.-Aided Des. Integr. Circuits Syst.*, vol. 23, no. 6, pp. 941–951, 2004.
- [3] K. Agarwal, M. Agarwal, D. Sylvester, and D. Blaauw, "Statistical interconnect metrics for physical-design optimization," *IEEE Trans. Comput.-Aided Des. Integr. Circuits Syst.*, vol. 25, no. 7, pp. 1273–1288, 2006.
- [4] P. Ghanta and S. Vrudhula, "Variational interconnect delay metrics for statistical timing analysis," in *Proc. 7th International Symposium on Quality Electronic Design ISQED '06*, pp. 6 pp.–, 2006.
- [5] Y. Bi, K. van der Kolk, N. van der Meijs, and D. Ioan, "Sensitivities computation of interconnect capacitances with respect to geometric parameters," *Proc. IEEE 17th Topical Meeting on Electrical Performance of Electronic Packaging*, 2008.
- [6] Y. Bi, N. van der Meijs, and D. Ioan, "Capacitance sensitivity calculation for interconnects by adjoint field technique," in *12th IEEE Workshop on Signal Propagation on Interconnects*, 2008.
- [7] A. Ruehli and P. Brennan, "Capacitance models for integrated circuit metallization wires," *IEEE J. Solid-State Circuits*, vol. 10, no. 6, pp. 530–536, 1975.
- [8] *SPACE Layout-to-Circuit Extractor*. <http://www.space.tudelft.nl>.